Combinatorial Approach to Identification of Catalysts for the Photoelectrolysis of Water

Michael Woodhouse,[†] G. S. Herman,[‡] and B. A. Parkinson*,[†]

Department of Chemistry, Colorado State University, Fort Collins, Colorado 80523, and Hewlett-Packard Company, Corvallis, Oregon 97330

Received March 10, 2005. Revised Manuscript Received June 7, 2005

A new simple and high-throughput combinatorial method to search for materials capable of the photoelectrolysis of water is presented. Ink jet printing is used to pattern metal oxide precursors (simple nitrate salts) onto conductive glass substrates. Subsequent pyrolysis yields electrodes with patterns of metal oxide compositions that, when immersed in an electrolyte, are easily screened for photoelectrolysis activity using a simple scanning laser system. Some promising metal oxide compositions were identified using this approach.

Introduction

Hydrogen obtained from renewable energy will be the fuel of choice either when fossil fuels become depleted or when the environmental consequences of burning fossil fuels are no longer acceptable. Direct photoelectrolysis of water using solar energy is the ideal method for producing hydrogen from a renewable, inexpensive and abundant raw material. The first steps toward this goal were taken more than 30 years ago by Fujishima and Honda when they demonstrated that crystalline rutile (TiO_2) electrodes, when illuminated with UV light, produced hydrogen from water without decomposition of the electrode.[1,2] Despite the promising start, there has been little progress toward an affordable, stable, and efficient method to photoelectrolyze water. Efficient photoelectrolysis of water has been achieved using expensive single-crystal III−V multijunction electrodes,[3] but their long-term stability and high cost remain problematic.

Due mainly to their inherent stability, semiconducting oxides are strong candidate materials for the ability to efficiently photoelectrolyze water. The ideal single-metal oxide photoanode or photocathode material will have a band gap around 1.6−2.0 eV. A photoelectrolysis system could also be efficient by coupling both a p-type and an n-type material to drive water photoreduction and photooxidation respectively, as was originally described by Nozik et al.,[4] where band gaps in the range of 0.8−1.2 eV for each material would be optimum. This approach, where annihilation of minority carriers at the ohmic contact generates the extra voltage or driving force for photoelectrolysis, also lowers the theoretical quantum yield by a factor of 2. However, this approach does have the advantage that two smaller band gap materials could be used, thereby extending the utilization of the solar spectrum into the near-infrared. The disadvantages of this approach are that the currents in the two electrodes must be matched for optimum efficiency and that two materials, rather than just one, need to be discovered and optimized.

A material will also need to be affordable and stable under illumination in aqueous electrolytes and be catalytic for the evolution of oxygen or hydrogen from water in order to minimize overpotential losses. The material must also have conduction and valence band energies negative of the water reduction potential and positive of the water oxidation potential, respectively. No such material or materials have been identified thus far. However, such a material will likely be composed of multiple metals, each of which contributes to the required special properties. High-temperature superconductivity is a good example of a special property requiring multicomponent materials. The oxide with the highest known transition temperature contains four metals ($HgBa_2CaCu_2O_{6+}\delta$, $T_c = 125$ K). Since our present theoretical knowledge is insufficient to a priori calculate the behavior of such complex systems, empirical methods will be necessary to identify the best material for efficient water photoelectrolysis. Thousands, or perhaps hundreds of thousands, of mixed metal oxide photocatalyst compositions may need to be produced and tested for efficiency and corrosion resistance until an effective material is discovered.

The recent development of combinatorial methods provides tools to speed the discovery process when a large number of candidate materials need to be synthesized and screened for the property of interest.[5] Combinatorial methods have been applied to optimize oxide materials for use as phosphors,[6−9] gate dielectrics,[10] and fuel cell catalysts.[11,12] The MacFarland group has demonstrated the electrochemical

* Corresponding author.
[†] Colorado State University.
[‡] Hewlett-Packard Company.

(1) Fujishima, A.; Honda, K. *Bull. Chem. Soc. Jpn.* **1971**, *44*, 1148.
(2) Fujishima, A.; Honda, K. *Nature* **1972**, *238*, 37.
(3) Khaselev, O.; Turner, J. A. *Science* **1998**, *280*, 425.
(4) Nozik, A. J. *Appl. Phys. Lett.* **1977**, *30*, 567.
(5) Reddington, E.; Sapienza, A.; Gurau, B.; Viswanathan, R.; Sarangapeni, S.; Smotkin, E. S.; Mallouk, T. E. *Science* **1998**, *280*, 1735.
(6) Wang, J.; Yoo, Y.; Gao, C.; Takeuchi, I.; Sun, X.; Chang, H.; Xiang, X.-D.; Schultz, P. G. *Science* **1998**, *279*, 1712.
(7) Sun, X.-D.; Gao, C.; Wang, J.; Xiang, X.-D. *Appl. Phys. Lett.* **1997**, *70*, 3353.

10.1021/cm050546q CCC: $30.25
Published on Web 07/22/2005

deposition of metal oxide compositions using robotics to plate and screen individually created materials and have looked at water photooxidation catalysts using multiplexed photoelectrochemical cells.[13]

Herein we report a novel high-throughput combinatorial search strategy to identify multicomponent metal oxide materials with suitable band gaps and band positions for water photoelectrolysis operating as either a photoanode or a photocathode. Our combinatorial search strategy uses ink jet printing of overlapping patterns of soluble metal nitrate salts, as metal oxide precursors, onto a conductive glass substrate. Metal nitrates decompose to form metal oxides, oxygen, and NO_2 by heating at relatively low temperatures.

The low cost, speed, and versatility of ink jet printing have made it attractive for combinatorial searches for fuel cell catalysts,[5] organic device combinations,[14] and biomaterials.[15] We feel that our approach has several major advantages over previous combinatorial search strategies for identifying oxide photoelectrolysis materials. First, we can create a continuous variation of composition across our samples to produce a plethora of compositions in each experiment. Second, we are not limited to materials that can be electrodeposited, and third, we do not need custom-engineered robotic devices but are using simple, inexpensive off-the-shelf items for both creating and screening our library. Finally, we are directly testing our compositions under the same conditions to be used in a realistic photoelectrolysis device (e.g., we do not use sacrificial reagents in our electrolyte and we illuminate our samples with visible wavelength radiation).

Experimental Section

Flourine-doped tin oxide coated glass (8-ΩR, 3.0 mm thickness) was obtained from Pilkington Industries and cut into 3 in. × 3 in. squares. The glass was soaked in an isopropyl alcohol/KOH base bath for a minimum of 30 min followed by rinsing with copious amounts of distilled water and ethanol. $Fe(NO_3)_3$, $Cu(NO_3)_2$, $CsNO_3$, $Nd(NO_3)_3$, $Co(NO_3)_2$, and $Al(NO_3)_3$ were obtained from Fisher Scientific (Fe), Strem (Cu and Nd), Alfa Aesar (Co and Cs), and Baker Chemical (Al) and all were analytical reagent grade. Solutions of the appropriate metal nitrate salt (0.35 M) with NH_4NO_3 (0.6 M) and HNO_3 (0.015 M) were injected into empty Hewlett-Packard 1220C DeskJet black ink jet printer cartridges. The cartridges were then manually primed using a commercially available kit from ABC Printer Repair and the cleaning cycle was run on each cartridge to ensure that printing was uniform. The SnO_2:F glass was taped to a piece of printer paper and patterns of nitrate salts were then sequentially printed for each metal. The metal salt solutions were often reprinted up to three times to achieve the appropriate metal oxide thickness.

The printed metal patterns were then fired at 500 °C for 24 h in a ThermoLyne Type 1300 furnace to decompose the metal nitrates into metal oxides. The metal oxide coated conductive glass was then connected as the working electrode in a two-electrode configuration with a Princeton Applied Research 174A Potentiostat. A loop of Pt wire around the perimeter of the printed substrate served as both the reference and counter electrodes. A 0.500 M NaOH solution was the electrolyte. A positive or negative bias was applied to screen for photoanode or photocathode materials, respectively. The sample was irradiated with the 514.5-nm line of an Ar^+ laser, the 532 nm line of a solid state frequency doubled YAG laser (BWN-532-20-E), or the 632.8 nm line of a Melles Griot 05-LHR-991 HeNe laser. The resulting photocurrent from the photoelectrochemical cell was measured with a Stanford Research Systems SR530 Model Lock-In Amplifier and a PTI model OC4000 chopper operating at 13 Hz. A program written with Labview software controlled the rastering of the laser over a selected region of the substrate by applying stepwise voltages to a two-mirror galvanometer (CLS-200 from Intelite, Inc.) and recording the subsequent photocurrent at each pixel (typically resulting in a 140 × 140 matrix for each scan). X-ray diffraction was done using the Cu Kα line from a Bruker D8 Discover glancing angle X-ray diffractometer. SEM images were taken with a field emission JEOL 6500F. Photocurrent spectroscopy was done using an apparatus that has been described previously.[16]

Results and Discussion

Our first task was to optimize printing procedures by printing thickness gradients of a single component and measuring the photocurrent. Figure 1A shows a simple rectangular gradient pattern that was printed onto SnO_2:F coated glass with 0.35M $Fe(NO_3)_3$. α-Fe_2O_3 has previously been shown to have some activity for water photooxidation and so it was a logical material for our initial studies.[17,18] The simple printed pattern was printed over once, twice, and three times to determine the number of times to overprint the metal nitrate solution in order to optimize the photocurrent signal. Thin film X-ray diffraction was used to verify that α-Fe_2O_3 is the phase produced by pyrolyzing ferric nitrate at 500 °C. A photograph of the substrate after printing and firing at 500 °C is shown in Figure 1B. The electrode/substrate was then immersed in a 0.5M NaOH solution with an applied bias of 0.5 V with respect to the platinum counter electrode in the same solution. A false color photocurrent scan, produced by scanning the 514 nm line of a chopped Ar ion laser over the immersed substrate, is shown in Figure 1C. The figure demonstrates that if the coating is too thin, then not much of the incident light is absorbed (1X scan). If the coating is too thick, the photogenerated carriers are created too far away from the metal oxide/solution interface and recombine before they can be transported to the interface (far end of 3X scan). The photocurrent scan reveals that the optimum thickness occurs about two-thirds of the way up

(8) Danielson, E.; Devenney, M.; Giaquinta, D. M.; Golden, J. H.; Haushalter, R. C.; McFarland, E. W.; Poojary, D. M.; Reaves, C. M.; Weinberg, W. H.; Wu, X. D. *Science* **1998**, *279*, 837.
(9) Danielson, E.; Golden, J. H.; McFarland, E. W.; Reaves, C. M.; Weinberg, W. H.; Wu, X. D. *Nature* **1997**, *389*, 944.
(10) Dover, R. B. v.; Schneemeyer, L. F.; Fleming, R. M. *Nature* **1998**, *392*, 162.
(11) Jaramillo, T. J.; Ivanovskaya, A.; McFarland, E. W. *J. Comb. Chem.* **2002**, *4*, 17.
(12) Cong, P.; Doolen, R. D.; Fan, Q.; Giaquinta, D. M.; Guan, S.; McFarland, E. W.; Poojary, D.; Self, K.; Turner, H. W.; Weinberg, W. H. *Angew. Chem., Int. Ed.* **1999**, *38*, 484.
(13) Baeck, S. H.; Jaramillo, T. F.; Brandli, C.; McFarland, E. W. *J. Comb. Chem.* **2002**, *4*, 563.
(14) Sirringhaus, H.; Kawase, T.; Friend, R. H.; Shimoda, T.; Inbasekaran, M.; Wu, W.; Woo, E. P. *Science* **2000**, *290*, 2123.
(15) MacBeath, G.; Schreiber, S. L. *Science* **2000**, *289*, 1760.
(16) Takeda, N.; Parkinson, B. A. *J. Am. Chem. Soc.* **2003**, *125*, 5559.
(17) Iwanski, P.; Curran, J. S.; Gissler, W.; Memming, R. *J. Electrochem. Soc.* **1981**, *128*, 2128.
(18) Leygraf, C. H.; Henderwerk, M.; Somorjai, G. A. *J. Phys. Chem.* **1982**, *86*, 4484.

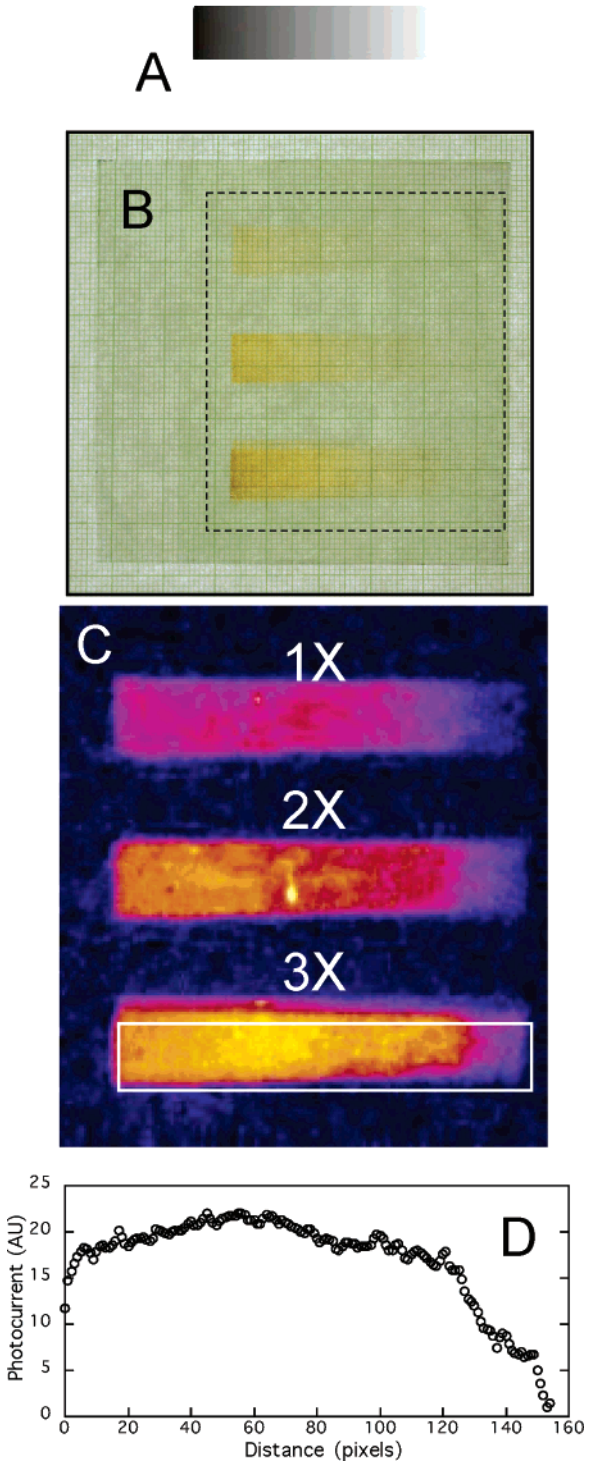

Figure 1. Overprinting a gradient pattern to optimize the metal oxide thickness. A. Rectangular gray scale gradient used to template the printing of the α-Fe_2O_3 precursor. B. Photograph of the gradient pattern in A that was printed one, two, and three times on SnO_2:F coated glass (graph paper underneath has 1 cm large squares). C. A false color photocurrent image of the region inside the dotted rectangle of B displaying IPCE values generated by scanning a 514.5 nm laser over the surface in a 0.5 M NaOH solution. D. Line profile obtained by averaging the IPCE values along the length of the rectangle outlined over the 3X printed gradient.

on the pattern that was been overprinted three times. Figure 1D shows a average photocurrent cross section for the region enclosed by the white rectangle in Figure 1D where the maximum in the photocurrent response is clearly seen 50−60 pixels from the end. This corresponds to an average thickness of about 12 nm of α-Fe_2O_3.

Once the concentration of solution in the ink jet cartridges and the number of overprints was optimized, we turned our attention to printing ternary and quaternary composition gradients. A significant advantage of printing the continuous composition gradients is that the effects of doping small amounts of different elements into a particular oxide can be simultaneously examined over a large range of doping levels by controlling the printing gradient—a useful property to examine as small amounts of added dopants have been shown to dramatically influence the photoactivity of metal oxide photoelectrodes.[19,20] Linear, exponential, or other gradient patterns can be used depending on the drawing program and the printer driver software. However, it must be kept in mind that the gradients produced by an ink jet printer are produced by variation in the density of individual ink dots and so are not continuous on a microscopic scale. Overprinting several times with a less concentrated solution, as was done in the thickness study discussed above, is one way to make the printed pattern more continuous, although regions of very light printing may have widely separated individual dots. Upon heating, the nitrate salts will first dehydrate and then melt and decompose, resulting in mixing of the elements.

Our initial high-throughput approach involves screening four metals, three at a time, in triangular patterns that represent the faces of an unfolded tetrahedron (Figure 2A) akin to the pattern used by Mallouk et al. for printing mixtures of precious metals for screening as fuel cell catalysts.[5] The unfolded tetrahedron pattern represents the four ternary faces of the three-dimensional tetrahedral four-component phase diagram.

The number of metal combinations to be screened can be enormous (there are at least 60 potentially useable metals in the periodic table, resulting in $>60^3$ or 216000 combinations for three components and $>60^4$ or almost 13 million for four). To reduce the number of combinations, we use some intuitive guidance to aid in selecting promising combinations. We can very loosely classify metals into one of four categories according to their potential role in a photoelectrode material; structural (e.g., Ti, W, Zr, Ta, Si, Mo, Nb, Hf, In, Sn, Ga, Y, Sc), light absorbing (e.g., Fe, Cr, V, Co, Mn, Ni, Cu, and some rare earths such as Ce), catalytic (e.g., Ru, Rh, Pd, Pt, Ir, Os, Re, Ni), and ionic charge compensators (e.g., Ca, Sr, Ba, Mg, Zn, Cd, Li, Na, K, Rb, Cs). (We are purposely avoiding toxic metals such as Pb, Tl, Cd, and Hg since we envision large-scale implementation of any discovered photocatalyst and we want to avoid the damaging environmental consequences of using these metals.) This intuitive guidance greatly reduces the number of possible combinations. For instance, it is not productive to try combinations of all high band gap materials (i.e., Ti−Zr−Si−Y oxides) since none of the elemental oxides absorb visible light and it is unlikely that the produced mixtures will either. It may, however, be useful to select multiple light absorbing metals that have complementary absorption bands in order to produce a material with better spectral overlap with the solar spectrum.

(19) Kennedy, J. H.; Anderman, M.; Shinar, R. *J. Electrochem. Soc.* **1981**, *128*, 2371.
(20) Houlihan, J. F.; Armitage, D. B.; Hoovler, T.; Bonaquist, D.; Madacsi, D. P.; Mulay, L. N. *Mater. Res. Bull.* **1978**, *13*, 1205.

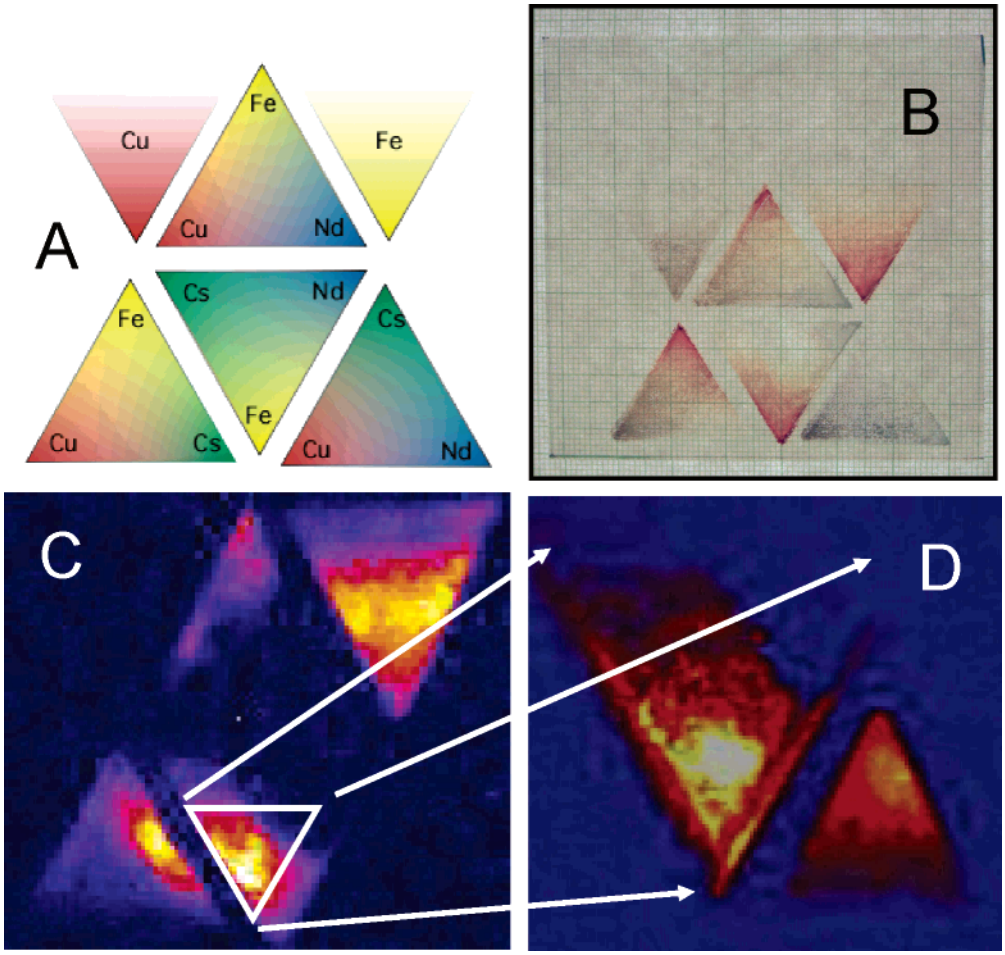

Figure 2. Printing and screening a four-metals-three-at-a-time pattern and a compositional zoom for the Fe−Cs−Nd−Cu system. A. False color template showing the positions and gradients used for printing the four metal precursor solutions. B. Photograph of the printed and fired film. Note the triangular internal standards of α-Fe_2O_3 and CuO (upper right and left, respectively) with thickness gradients (bottom to top) that are used as internal standards. C. False color photocurrent image of the film shown in B using 514.5 nm illumination under a 0.5 V bias in 0.5 M NaOH solution. D. Photocurrent scan at 514.5 nm of a triangular composition zoom in on the brightest area of the Fe−Cs−Nd triangle shown in C that has a maximum IPCE value approximately twice that of the α-Fe_2O_3 internal standard (smaller triangle to the lower right).

To date, we have printed and screened dozens of the four-metal-three-at-a-time patterns discussed above. Figure 2B shows a photograph taken after twice printing the pattern in 2A of Fe, Cu, Nd, and Cs and firing the film. Additional small triangles of α-Fe_2O_3 and CuO were printed in the upper left and upper right respectively with their thickness decreasing from bottom to top. We use these triangular areas as internal standards for the photocurrent screening since these materials show some n-type photoactivity for water oxidation (α-Fe_2O_3) and p-type activity for water reduction (CuO).[21] The α-Fe_2O_3 triangle "lights up" in screening scans with a positive applied bias (Figure 2C upper left triangle) whereas the CuO triangle lights up with a negative applied bias (not shown in this figure). The internal standards provide a check that our processing conditions are reproducible from run to run and serve as a benchmark for the photoactivity of the mixed phases printed in the main triangles. Areas showing considerably higher photocurrent, relative to the internal standards, then represent promising new compositions.

Figure 2C shows the results of screening the combination of Fe, Cu, Nd, and Cs with the same conditions used in Figure 1. We add a small electrical bias ($\pm$0.5 V) to reveal compounds that are effective light absorbers but may not be especially catalytic toward water oxidation (positive bias) or reduction (negative bias). The photocurrent scan (Figure 2C) reveals that adding Cs and Nd to Fe_2O_3 produces a composition with a photoresponse almost 2 times higher than the pure α-Fe_2O_3 internal standards (central triangle of Figure 2C). Although adding small amounts of Nd appears to enhance the photoresponse, too much Nd kills the photocurrent as indicated by the total loss of photocurrent near the Nd vertex. The Fe, Cu, Cs triangle also shows a respectable response along the Fe−Cs edge of the triangle.

Areas of the printed patterns that show promising photocurrent can be expanded by adjusting the printed pattern such that the composition at the vertexes of the newly printed triangle border the "hot spot" in the photocurrent map. Figure 2D shows an example of such a "zoom in" on the promising high photocurrent area of the Fe, Cs, Nd triangle from Figure 2C. Again an abrupt loss of photocurrent is visualized when the Nd content becomes too high. The zoom in technique allows further refinement of the composition of a promising photocatalyst. Rational methods can then be used for further compositional refinement. For example, a ternary composition that shows good light absorption, but poor current−

(21) Hardee, K. L.; Bard, A. J. *J. Electrochem. Soc.* **1977**, *124*, 215.

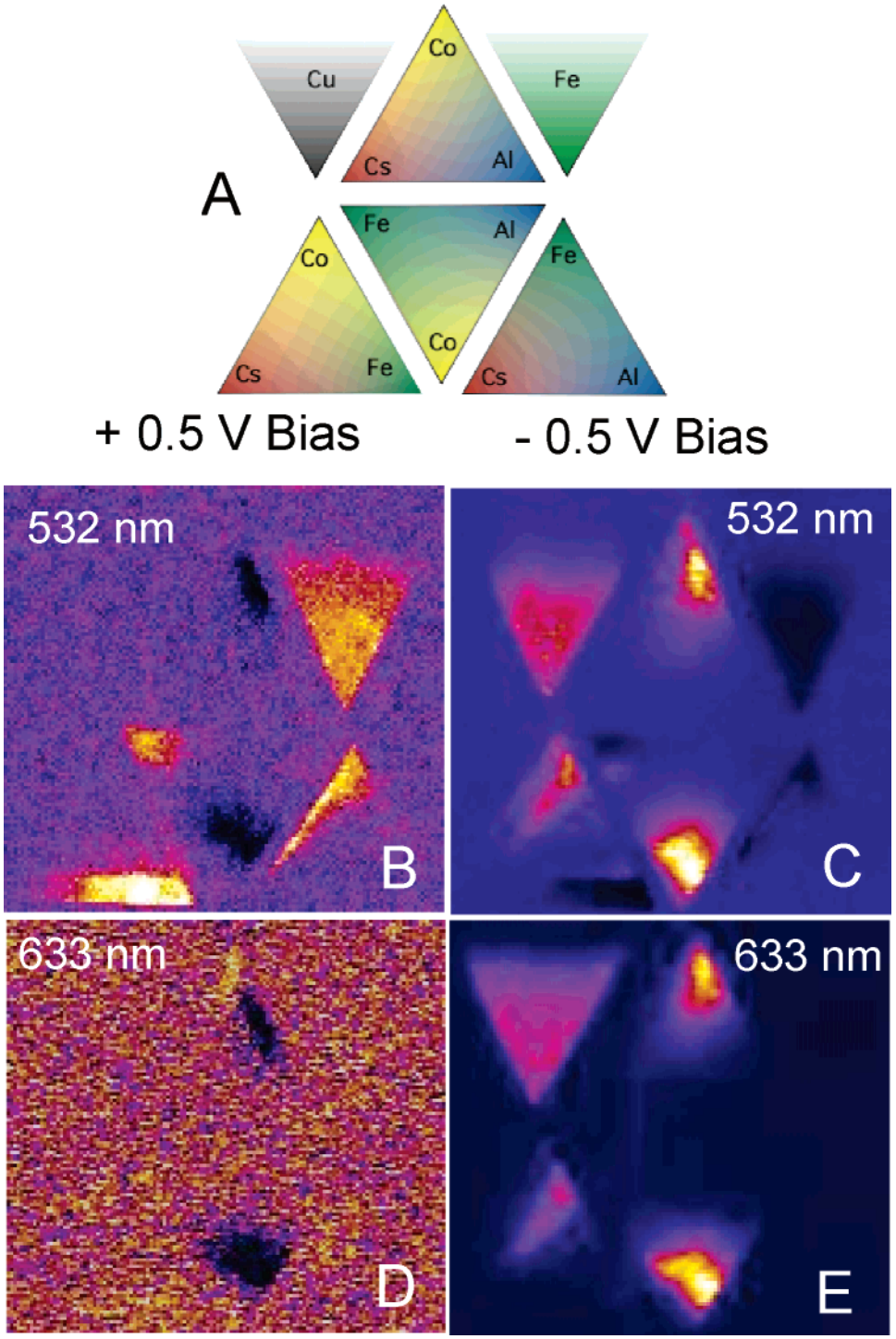

Figure 3. Printing and screening at two laser wavelengths and two different biases a four-metals-three-at-a-time pattern for the Fe−Cs−Co−Al system. A. False color template showing the positions and gradients used for printing the four metal precursor solutions. B. Laser screening scan at 532 nm with a 0.5 V bias in a 0.5 M NaOH solution. C. Same film scanned at −0.5 V. D. Same film scanned at 632 nm with a 0.5 V bias. D. Same film scanned at 632 nm with a −0.5 V bias. Refer to the text for a more complete description.

voltage behavior for water photoelectrolysis, will be printed with a constant composition and be overprinted with gradient patterns of combinations of catalytic metals. This method provides an entry into the very large four-component phase space.

Figure 3 shows the "four-metals-three-at-a-time" approach for Fe, Co, Al, and Cs. Figure 3A shows a color-keyed printing pattern. We have screened this combination at both 532 nm (2.33 eV) and 632.8 nm (1.96 eV) so that an initial spectral response is obtained, and at both positive and negative biases to highlight n-type and p-type materials. It can be seen in Figure 3B that illuminating the α-Fe_2O_3 internal standard with 532 nm light under a positive bias produces a response as does the Fe−Cs edge of the Fe−Cs−Co triangle. The Fe−Cs−Al triangle also generates a response but with the Al suppressing the photocurrent at even small amounts. The dark regions represent areas where the photocurrent is still in the cathodic direction despite the positive applied bias and correspond to the brightest areas of the 532 nm scan done at negative bias (as shown in Figure

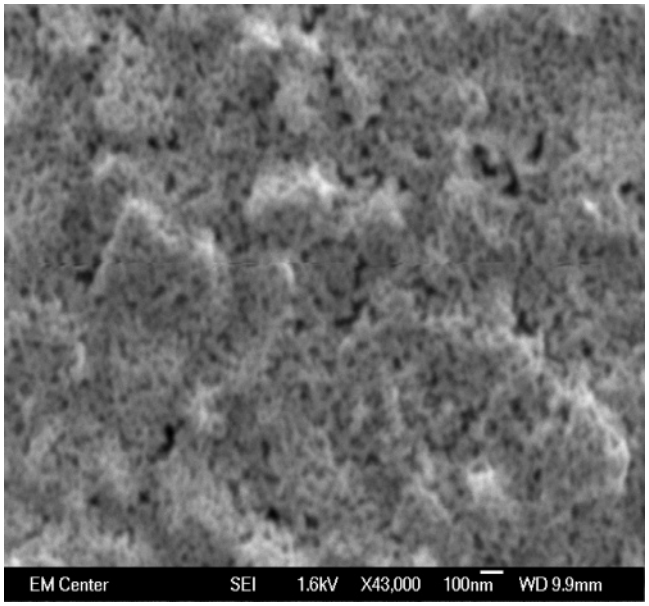

Figure 4. SEM image of the bright area shown in the photocurrent scan of Figure 2D showing that in this area the metal oxide film is a porous film overlaying the conductive SnO_2:F substrate.

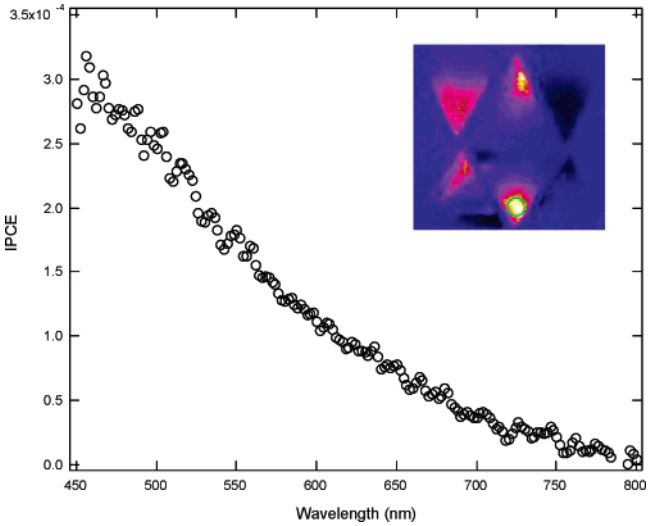

Figure 5. Photocurrent action spectrum measured in the area of the bright spot seen in Figure 3C and 3E and outlined with a green circle in the inset. The spectrum was measured in a 0.5M NaOH solution at a bias of −0.5 V.

3C where the Cu internal standard lights up). Areas of p-type photoresponse that are 2−2.5 times higher than pure CuO are identified in Figures 3C and 3E for the Co-rich regions of the Co−Al−Fe and Co−Al−Cs triangles. Scanning the sample using 632.8 nm laser light at positive bias (Figures 3D) produces no appreciable anodic photocurrent. One can only see noise and a small p-type response since this wavelength is below the band gap of α-Fe_2O_3 and other phases that are present. At negative bias the photocurrent image is similar to the image taken with 532 nm illumination, confirming that the new Co-containing phase has a band gap of less than 1.96 eV. We also repeated the 532 nm scan with no bias applied to the sample in order to verify that the cathodic photocurrent could still be generated. The photocurrent image had the same appearance as the images in Figure 3C and 3E but with a smaller maximum current value, demonstrating the strong p-type response of this new metal oxide composition and that it is apparently capable of a spontaneous water photoelectrolysis albeit at a very low efficiency.

Examination of the surface of the pyrolyzed samples with an optical microscope reveals that the surface can be heterogeneous and porous. Different areas of the surface appear microcrystalline, glassy, or even somewhat free of any deposits. Although the heterogeneity is perhaps not aesthetically pleasing, and points out that we are not producing the true triangular ternary phase diagram of the system, it is actually a virtue of our method. Since we screen only for the desired property, photoactivity, and the phase structure and composition of our eventual target material is not known in advance, a variety of microscopic morphologies produce more diverse possibilities from which an effective photocatalyst might be discovered. SEM imaging of smaller selected areas (Figure 4) reveals areas of porous microcrystalline deposits with a grain size of less than 100 nm.

Areas of the printed patterns that show promising photocurrent response can have their composition and morphology determined. A pure crystalline compound, mixtures of crystalline compounds, solid solutions of metal oxides, and amorphous oxide materials are all possible outcomes from mixing and pyrolysis of the printed precursors. Thin film X-ray diffraction can be used to examine crystalline phases that may be present as was used to identify CuO and Fe_2O_3 in the internal standards. Simply mixing larger amounts of the nitrate salt precursors and pyrolyzing them at the same temperature allows the preparation of larger samples for bulk analysis. Pyrolysis temperature is another important variable that will determine which phase or phases are produced; however, we are limited to a maximum temperature of 550 °C by the stability of the conducting glass substrate.

SEM coupled with EDX analysis can quantify the presence and proportion of the elements in a particular spot on the sample as was done on the area in Figure 3. More detailed characterization of the band gap of a promising composition can be obtained by measuring the photocurrent spectrum of that area of the triangle. Figure 5 shows the photocurrent spectrum of the area identified in the Co−Al−Fe triangle shown in Figure 3D and 3F (central triangle) and repeated as an inset in Figure 5. The photocurrent spectrum, taken in the area of the green circle in the inset of Figure 5, shows that this phase produces photocurrent at wavelengths out to about 785 nm or 1.58 eV. A band gap lower than ∼1.8 eV makes this material a candidate p-type material for a p−n photoelectrolysis system. Further and more detailed examination of the behavior and phase composition of this new material is currently underway and will be presented elsewhere.[22]

Any discovered materials must be configured to achieve useful energy conversion efficiencies. The low IPCE values (10^{-4} to 10^{-5}) measured for the phases in Figures 1, 2, and 3 is a result of the thin film of printed material allowing most of the light to pass through without being absorbed. This is because transitions involving d and f levels on the metal atoms, which impart color to the oxides, generally are

(22) Woodhouse, M.; Parkinson, B. A. In preparation.

forbidden transitions and do not have high absorption coefficients. The low absorption coefficients result in the incident light penetrating deep into the material and since the carrier mobilities in oxides are generally much lower than in conventional solar cell materials, recombination of photogenerated carriers occurs before they can reach the semiconductor/electrolyte interface. Even good single crystals of metal oxides have energy conversion efficiencies that are not useful due to their inherently short diffusion lengths.[23]

Problems of low light absorption and small carrier mobilities were overcome by the dye-sensitized nanocrystalline TiO_2 photovoltaic cell, also known as the Grätzel solar cell.[24] The light absorption was improved by creating a high surface area porous TiO_2 electrode so that the incident light traverses many dye/oxide interfaces. When light absorption does occur, the carriers are always created at the interface so that carrier diffusion lengths do not limit performance. The electron lifetime in the porous TiO_2 network was long enough that they could diffuse to the back contact and be collected as photocurrent. The Grätzel cell contains relatively cheap materials and has reached solar-to-electric conversion efficiencies of up to 11%[25] with a demonstrated stability over many thousands of hours.[26] We anticipate increasing the photoelectrolysis efficiency of any discovered materials either by combining them with nanocrystalline TiO_2 or by deploying them as nanocrystalline thin films. The coating on titanium dioxide will be only several nanometers thick or be made up of nanometer-sized particles so that photogenerated carriers will reach the electrolyte interface despite their low mobilities. Low absorption coefficients will not limit device efficiencies since the total path length of light through the absorbing oxide can be large enough to absorb virtually all of the incident solar light.

(23) Jarrett, H. S.; Sleight, A. W.; Kung, H. H.; Gilson, J. L. *J. Appl. Phys.* **1980**, *51*, 3916.
(24) Regan, B. O.; Gratzel, M. *Nature* **1991**, *353*, 737.
(25) Nazeeruddin, M. K.; Kay, A.; Rodicio, I.; Humphry-Baker, R.; Muller, E.; Liska, P.; Vlachopoulous, N.; Gratzel, M. *J. Am. Chem. Soc.* **1993**, *115*, 6382.
(26) Kohle, O.; Meyer, A.; Meyer, T.; Gratzel, M. *Adv. Mater.* **1997**, *9*, 904.

The "Grätzel configuration" also provides additional device efficiency advantages for a photoelectrolysis system. The high surface area results in lower microscopic current densities, thereby reducing overpotential losses for hydrogen and oxygen generation. Low current densities will also contribute to electrode stability since corrosion reactions are often multielectron. Backside illumination, rather than through the electrolyte, will reduce any scattering of incident solar radiation from evolving gas bubbles, a problem that plagues the most efficient front-side illumination photoelectrolysis devices.[3]

Conclusion

We have demonstrated a new high-throughput combinatorial method to search for materials capable of the photoelectrolysis of water. Ink jet printing was shown to be an inexpensive, rapid, and versatile method of patterning metal oxide precursors onto a conductive glass substrate. Subsequent pyrolysis yielded electrodes with patterns of metal oxide compositions that, when immersed in an electrolyte, could be easily screened for photoelectrolysis activity using a simple scanning laser system. We have shown that promising compositions can be identified using our approach. The throughput of a combinatorial search is limited by the slowest step in the process. In our case we have determined that the screening step is rate limiting. Higher laser power and/or building additional scanning systems can dramatically increase throughput for this step and both are currently being implemented in our lab. The knowledge base derived from the increasing number of printed and screened compositions should also begin to suggest new combinations and further refine the compositions and properties needed to solve this important problem.

Acknowledgment. We appreciate useful discussions with Dave Schut. M.W. acknowledges financial assistance from the Maciel Fellowship. Partial support from the DOE under Contract DE-F603-96ER14625 is also acknowledged.

CM050546Q